# Decoupling peroxyacetyl nitrate from ozone in Chinese outflows observed at Gosan Climate Observatory

**Jihyun Han[1*], Meehye Lee[1], Xiaona Shang[1], Gangwoong Lee[2], Louisa K. Emmons[3]**

[1]Department of Earth and Environmental Sciences, Korea University, Seoul, Republic of Korea

[2]Department of Environmental Science, Hankuk University of Foreign Studies, Yongin, Republic of Korea

[3]Atmospheric Chemistry Observations and Modeling Laboratory, National Center for Atmospheric Research (NCAR), Boulder, CO, USA

*now at: Korea Environment Institute, Sejong, Republic of Korea

Correspondence to: M. Lee (meehye@korea.ac.kr )

Submitted to Atmospheric Chemistry and Physics

December 2016

**Abstract**

We measured peroxyacetyl nitrate (PAN) and other reactive species such as $O_3$, $NO_2$, CO, and $SO_2$ with aerosols including mass, organic carbon (OC), and elemental carbon (EC) in $PM_{2.5}$ and $K^+$ in $PM_{1.0}$ at Gosan Climate Observatory in Korea (33.17°N, 126.10°E) during October 19 to November 6, 2010. PAN was determined through fast gas chromatography with luminol chemiluminescence detection at 425 nm every 2 min. The PAN mixing ratios ranged from 0.1 (detection limit) to 2.4 ppbv with a mean of 0.6 ppbv. For all measurements, PAN was unusually better correlated with $PM_{2.5}$ (Pearson correlation coefficient, $\gamma = 0.79$) than with $O_3$ ($\gamma = 0.67$). In particular, the $O_3$ level was highly elevated with $SO_2$ at midnight, along with a typical midday peak when air was transported rapidly from the Beijing areas. The PAN enhancement was most noticeable during the occurrence of haze under stagnant conditions. In Chinese outflows slowly transported over the Yellow Sea, PAN gradually increased up to 2.4 ppbv at night, in excellent correlation with a concentration increase of $PM_{2.5}$ OC and EC, $PM_{2.5}$ mass, and $PM_{1.0}$ $K^+$. The high $K^+$ concentration and OC/EC ratio indicated that the air mass was impacted by biomass combustion. This study highlights PAN decoupling with $O_3$ in Chinese outflows and suggests PAN as a useful indicator for diagnosing continental outflows and assessing their perturbation on regional air quality in northeast Asia.

Key words: PAN, $O_3$, $PM_{2.5}$, Chinese outflow, Haze, Biomass combustion

## 1. Introduction

At the surface, ozone is primarily photochemically produced, and the contribution from the stratosphere is generally small. Ozone is formed through reactions of various precursors such as CO, $CH_4$, volatile organic compounds (VOCs), and $NO_x$ (e.g., Brasseur et al., 1999; Jacob, 2000; Nielsen et al., 1981). Likewise, peroxyacetyl nitrate (PAN) is a secondary product of urban air pollution and a significant oxidant in the atmosphere (e.g., Hansel and Wisthaler, 2000; La Franchi et al., 2009; Lee et al., 2012; Liu et al., 2010; Roberts et al., 2007). PAN is solely produced by the photochemical reaction between the peroxyacetyl radical and nitrogen dioxide, and the peroxyacetyl radical is derived from the OH oxidation or photolysis of VOCs such as acetaldehyde, methylglyoxal, and acetone (e.g., Fischer et al., 2014; La Franchi et al., 2009; Lee et al., 2012). For this reason, PAN is a very useful indicator of photochemical air pollution. As thermal decomposition is a major PAN sink in the troposphere (Beine et al., 1997; Jacob, 2000; Kenley and Hendry, 1982; Talukdar et al., 1995), the lifetime of PAN depends on temperature. For example, the PAN lifetime is ~5 years at −26°C and 1 h at 20°C (Fischer et al., 2010; Zhang et al., 2011). At high altitudes above ~7 km, photolysis becomes the most important loss process for PAN (Talukdar, et al., 1995). Because of low solubility, PAN is not prone to atmospheric removal, thereby being more efficiently transported to the free troposphere (e.g., Zhu et al., 2017). Thus, PAN can be an indicator of $NO_y$ concentration in the free troposphere and a guide for the long-range transport of $NO_x$ in remote regions (Jacob, 1999).

In the past decades, PAN was measured not only in urban areas (Aneja et al., 1999; Gaffney et al., 1999; Grosjean et al., 2002; Lee et al., 2008; Tanimoto et al., 1999; Zhang et al., 2014) but also in background regions (Fischer et al., 2011; Kanaya et al., 2007; Lee et al.,

2012; Tanimoto et al., 2002), onboard aircraft (Tereszchuk et al., 2013), and ships (Roberts et al., 2007). PAN concentrations were in the range of a few ppbv in urban areas close to VOCs and $NO_x$ sources (Lee et al., 2008; Zhang et al., 2011). In the most remote regions, PAN concentrations were generally in the range of a few pptv (Gallagher et al., 1990; Mills et al., 2007; Muller and Rudolph, 1992; Staudt et al., 2003).

Although $NO_x$ concentration has recently declined in China (Gu et al., 2013; Liu et al., 2016a; Krotkov et al., 2016), $NO_x$ and VOCs have gradually increased in East Asia, particularly China during the last couple of decades (Akimoto, 2003; Liu et al., 2010; Ohara et al., 2007; Zhao et al., 2013). It led to an increase in the concentrations of photochemical byproducts such as PAN and $O_3$ not only in East Asia (Liu et al., 2010; Wang et al., 2010; Zhang et al., 2009; Zhang et al., 2011; Zhang et al., 2014) but also in North America (Fischer et al., 2010; Fischer et al., 2011; Jaffe et al., 2007; Zhang et al., 2008). These results were also demonstrated by the GEOS-Chem model (Zhang et al., 2008). In addition to urban plumes, PAN was reported to be enhanced by biomass combustion (Alvarado et al., 2010; Coheur et al., 2007; Zhu et al., 2015; Zhu et al., 2017), such as open burning and use of biofuel, which is used to take place often in China after crop harvesting (Cao et al., 2006; Duan et al., 2004). Recent satellite studies have also observed the increased PAN in plumes associated with anthropogenic emissions in eastern China and boreal fires in Siberia (Zhu et al., 2015; Zhu et al., 2017). In this context, PAN is a useful tracer for estimating the impact of Chinese outflows on regional air quality in the northern Pacific region.

Gosan Climate Observatory (GCO) is an ideal place to monitor Asian outflows and their transformation and to estimate their impact on air quality over the northern Pacific region (Lee et al., 2007; Lim et al., 2012). In the present study, PAN was first measured continuously at GCO to characterize its variation and source in relation to $O_3$ and to

94 understand the influence of Chinese outflows on the regional air quality.

95

96 **2. Experiments**

97

98 PAN measurements were conducted at GCO (33.17°N, E126.10°E) on Jeju Island from
99 October 19 to November 6, 2010. GCO is located on a cliff at the western edge of Jeju Island.
100 PAN was determined through fast gas chromatography (GC) with luminol
101 chemiluminescence detection, which is described in detail elsewhere (Gaffney et al., 1998;
102 Lee et al., 2008; Marley et al., 2004). Here, we briefly describe the measurement method.
103 Ambient air was pumped through a 1.6-m PFA tubing (1/4 inch outer diameter) from the
104 roof of the two-story container into a six-port injection valve (Cheminert C22, Valco
105 Instruments (Houston, TX, USA)) at 100 ml/min controlled by Mass flow controller (Lee et
106 al., 2012; Lee et al., 2008). The residence time of the inlet was less than 2 seconds. PAN and
107 $NO_2$ (and peroxypropyl nitrate (PPN) if present) were separated along a 10-m capillary GC
108 column (DB-1, J&W Scientific, Folsom, CA, USA), whose end was connected to a luminol
109 cell where the column effluent reacted with luminol, giving off luminescent light (Lee et al.,
110 2008; Lee et al., 2012). The concentrations of PAN and other species were determined from
111 the chemiluminescence signals detected by a gated photon counter (HC135-01, Hamamatsu,
112 Bridgewater, NJ, USA) at 425 nm, which was set at 800 V and operated at room temperature
113 (Gaffney et al., 1998; Lee et al., 2012; Lee et al., 2008).
114 PAN was calibrated against standards synthesized by the nitration of peracetic acid in n-
115 tridecane (Gaffney et al., 1984; Gregory, 1990; Lee et al., 2008). A few microliter aliquots of
116 standard solution were injected through an injection valve and then mixed with zero air
117 (99.999 %) in a 5 L Tedlar bag. After being left for a few minutes for equilibrium, it was

injected into GC-luminol instrument and NOx chemiluminescence instrument with a molybdenum converter (42C, Thermo Electron Corporation, Franklin, MA, USA). The calibration was completed within 5 minutes to prevent thermal decomposition of the PAN (Kourtidis et al., 1993; Lee et al., 2008). These calibration procedures were carried out on the assumption that the PAN was completely converted to NO in the molybdenum converter. The detection limit of PAN defined by 3σ of the lowest standard was no greater than 100 pptv (Lee et al., 2008). The overall measurement uncertainty and precision was estimated to be 16 % and 5%, respectively (Lee et al., 2012). $NO_x$ instrument was calibrated with NO standard gas.

Gaseous species including $O_3$, NO, $NO_2$, CO, and $SO_2$ were measured by UV absorption, chemiluminescence with a molybdenum converter, non-dispersive infrared, and pulse UV fluorescence method, respectively (NIER, 2016a). The measurements were made in compliance with guidelines for installation and operation of air pollution monitoring network (NIER, 2016b). Calibration was conducted before and after the experiment, following the regular checkup procedure. Detection limits of $O_3$, $NO_x$, CO, and $SO_2$ are 2 ppb, 0.1 ppb, 50 ppb, 0.1 ppb, respectively (NIER, 2016b). It should be noted that $NO_2$ concentration reported in the present study is actually the sum of $NO_2$ and NOz species due to well-known positive artifact of molybdenum convertor. PAN is one of the major NOz species and the ratio of PAN to $NO_2$ was 12 ± 7 % for the whole measurements.

Aerosol species, including $PM_{2.5}$ mass and $PM_{2.5}$ OC and EC were measured and recorded along with meteorological parameters (relative humidity, temperature, and wind direction and speed). Water-soluble ions of $PM_{1.0}$ were collected by a particle-into-liquid sampler (PILS) and analyzed by ion chromatography. The detailed results of the aerosol measurements can be found in Shang et al. (2017).

For the air parcel at 850 m a.s.l, the three-day backward trajectories were calculated every

hour using NOAA Air Resources Laboratory (ARL) Hybrid Single-Particle Lagrangian Integrated Trajectory (HYSPLIT) model (version 4) (Draxler and Rolph, 2012; Rolph, 2012, http://www.arl.noaa.gov/ready/hysplit4.html). In addition, $O_3$ and PAN concentrations were calculated using a global chemistry model, the Community Atmosphere Model with Chemistry (CAM-Chem), a component of the Community Earth System Model (CESM) (Lamarque et al., 2012; Tilmes et al., 2015). The CAM-chem results shown here follow the configuration used for the HTAP2 (Hemispheric Transport of Air Pollution, Phase 2) intercomparison (e.g., Stjern et al., 2016). CAM-chem is nudged to observed meteorology (GEOS-5) to reproduce the actual period of the observations (Oct 2010). The emissions used in the model are the HTAP2 inventory (Janssens-Maenhout, et al., 2015), which include the "MIX" Asian emissions inventory. Biomass burning emissions are from the Global Fire Emissions Database (GFED3) (Randerson et al., 2013).

## 3. Results

In the present experiments, PAN concentrations range from 0.1 to 2.4 ppbv, with an average of 0.6 ppbv. This mean value is lower than those observed in other Asian megacities: Beijing (1.41 ppb in the summer), Pearl River Delta region (1.32 ppb in the summer), and Seoul (0.8 ppb in the early summer); similar to those of suburban areas in China, e.g., Lanzhou (0.76 ppb in the summer); and higher than those of urban and rural sites in Japan, e.g., Tokyo (up to 0.6 ppb in the fall), Rishiri Island (~0.5 ppb in spring) or in the western coast of the US, e.g., Sacramento (0.45 ppb in the summer), Mt. Bachelor (0.144 ppb in the spring and early summer), off the western coast of the US (0.65 ppb in the spring), and over the remote North Pacific (total PAN < 0.3 ppb in spring) (Bertram et al., 2013; Fischer et al.,

2011; La Franchi et al., 2009; Lee et al., 2008; Roberts et al., 2004; Tanimoto et al., 1999; Tanimoto et al., 2002; Wang et al., 2010; Zhang et al., 2009; Zhang et al., 2011). Because the PAN lifetime is greatly dependent on temperature, its concentration decreases with increasing distance from the source regions. The PAN concentrations calculated in this study thus lie in-between the levels for the East Asian megacities and the northern Pacific. The distributions of all measured species, including PAN and $O_3$, are presented in Fig. 1. In particular, there are several periods characterized by high concentrations of PAN, $O_3$, and $PM_{2.5}$. In terms of PAN, four periods are particularly interesting (Fig. 1). High $O_3$ concentrations were observed during October 31–November 2 [episode 1] but did not coincide with high PAN concentrations. During October 28–29 [episode 2], $NO_2$ was noticeably increased. In comparison, PAN and $O_3$ concentrations were both high during October 20–21 [episode 3] and November 4–5 [episode 4]. Episodes 3 and 4 are characterized by haze, while episodes 1 and 2 are characterized by urban influence in the Korean and Beijing outflows, respectively. Haze is reported by Korea Meteorological Administration (KMA) as a meteorological phenomenon when visibility is 1~ 10 km and relative humidity is less than 75 %.

In the present study, PAN correlates reasonably well with $O_3$ ($\gamma$ = 0.67) and even better with $PM_{2.5}$ ($\gamma$ = 0.79). In general, $O_3$ and PAN exhibit typical diurnal variation with a maximum recorded in the afternoon, which results in a good correlation between the two (Brasseur et al., 1999; Gaffney et al., 1999; Ridley et al., 1990; Schrimpf et al., 1995; Wang et al., 2010). In this study, however, the $O_3$ peak was often found in the early morning and late afternoon for several days (Fig. 1). Observing the diurnal variations in the entire PAN concentration measurement set (Fig. 2), the maximum was clearly recorded in the morning with the highest outliers, which is rather similar to that of $PM_{2.5}$. The diurnal pattern of $NO_2$ shows little variation, even though its concentrations were increased in the morning along

190 with PAN. This first measurement of PAN at GCO reveals that PAN is not always coupled
191 with $O_3$, which was not typically observed at remote sites in previous studies (e.g., Fischer et
192 al., 2010; Lee et al., 2012).
193
194 **4. Discussion**
195 **4.1. Decoupling of PAN from $O_3$**
196
197 To examine the detailed mechanism of the decoupling of PAN from $O_3$, the daily
198 maximum concentrations of PAN and $O_3$ were further explored. The recorded daily PAN
199 maxima were generally in good correlation with $O_3$, albeit the relationship did not seem to
200 hold at high concentrations of PAN and $O_3$ (Fig. 3). The daily maxima were then categorized
201 into four groups according to the time when each $O_3$ and PAN maximum was recorded: "$O_3$
202 day-PAN day", "$O_3$ day-PAN night", "$O_3$ night-PAN day", and "$O_3$ night-PAN night". The
203 day interval started from 08:00 and ended at 18:00 (local time), based on the times of sunrise
204 and sunset during the experiment period. While the high PAN concentrations were associated
205 with the "$O_3$ day-PAN day" group (cross symbols in Fig. 3), the enhanced $O_3$ concentration
206 was recorded in the "$O_3$ night-PAN night" group (star symbols in Fig. 3). The "$O_3$ night-PAN
207 night" group unexpectedly held more data points than the "$O_3$ day-PAN day" group, even
208 though the "$O_3$ night-PAN night" group concentrations were lower (Fig. 3). In addition, there
209 were several days classified in the "$O_3$ night-PAN day" (marked by diamond) and "$O_3$ day-
210 PAN night" groups, but with less frequency and lower concentrations. These results indicate
211 that the decoupling of PAN from $O_3$ was primarily due to the elevated concentrations of $O_3$
212 and PAN at night. While PAN reached the maximum during the day on Oct 20 and Nov 5,
213 their concentrations were increased from the previous day through the night. The four high

PAN and $O_3$ episodes identified in this study fall under the category of "$O_3$ night-PAN night" or "$O_3$ day-PAN day". These two cases will be further examined to identify the chemical and physical processes responsible for PAN being decoupled from $O_3$, instead of being coupled with $PM_{2.5}$. The overall characteristics of the four episodes are summarized in Table 1.

### 4.2. Export of $O_3$ from Asian continents (episodes 1 & 2)

High $O_3$ concentrations were encountered around midnight on three consecutive days from October 31 to November 2 (episode 1), during which $SO_2$ reached its maximum concentration (Fig. 1). The backward trajectories of air masses revealed that air passed through the Beijing area during this period (Fig. 4). The strong wind (13.5 m/s on average) implies that it would take about a day for air mass leaving Beijing area to arrive at GCO. The recorded $O_3$ maximum (80.6 ppbv) was concurrent with the PAN maximum (0.9 ppbv) around midnight on November 1st (Fig. 1). All these results indicate that the air was heavily influenced by outflow from the Beijing area, as previously hypothesized (Lim et al., 2012), and that the nighttime enhancement of $O_3$ and PAN with $SO_2$ resulted from the fast transport of urban plumes from China.

In previous studies, the nighttime enhancement of $O_3$ was observed at GCO (e.g., Lee et al., 2007) in association with pollutant-laden air coming from Beijing. Similarly, Banta et al. (1998) pointed out that the evening $O_3$ maximum was due to long-range transport of $O_3$ from nearby urban areas. Wang et al. (2011) reported that the $O_3$ lifetime was about two days in East China during the summer, which is sufficient for $O_3$ to travel to GCO but not for PAN due to its short lifetime. Therefore, the nighttime maximum of $O_3$ can be attributed to the export of $O_3$ from megacities in China, causing PAN to be decoupled from $O_3$. Because the overall correlation between $O_3$ and PAN was the best with the highest$\Delta O_3/\Delta$PAN among all

cases discussed in this study (Fig. 5a), episode 1 likely represents an event of rapid transport from the Beijing area.

Another night maximum of $O_3$ was recorded on October 29. Note that $NO_x$ was highly elevated with the lowest $SO_2$ concentrations during October 28–29 (episode 2) (Fig. 1). In episode 2, $O_3$ concentrations were much lower and poorly correlated with those of PAN, compared to episode 1. Instead, PAN was best correlated with $NO_2$ with the highest $\Delta NO_2/\Delta PAN$ among all episodes (Fig. 5a, b). In this case, air masses passed through the Korean Peninsula, carrying low $O_3$ being titrated by high $NO_x$ (Brasseur et al., 1999; Jacobson, 2005). These two episodes illustrate the export of urban plumes in northeast Asia region, which are distinguished by relative enhancement of reactive gases including $O_3$, PAN and $NO_x$, depending on the origin and aging of air masses.

### 4.3. PAN enhancement upon occurrence of haze (episodes 3 & 4)

In this study, two haze events were observed in the very beginning (October 20–21; episode 3) and the end of the study period (November 4–5; episode 4). As the nighttime $O_3$ peak was attributed to the transport from nearby urban areas to Jeju Island, the two haze episodes were also observed in association with continental outflows. The first haze event occurred on October 18th and lingered until October 21st, during which $O_3$ concentrations were gradually elevated. A second peak was recorded around midnight of October 19th and 20th, and the maximum was reached in the afternoon of October 20th (Figs. 1 and 3). In this episode, the maximum concentrations of $O_3$ and PAN were 78.9 ppbv and 2.0 ppbv, respectively, on October 20th, when the highest $NO_2$ concentration (12.7 ppbv) was observed under low wind speed (6.6 m/s daily average). The air mass trajectories suggest the influence

of the Korean Peninsula, particularly the Seoul metropolitan area, in addition to East China (Fig. 4).

In the second haze event (episode 4), an air mass was slowly transported from East China, including the Jiangsu province, under stagnant condition which was developed by an anticyclone system (Fig. 4). We measured the highest concentrations of all aerosol species including the $PM_{2.5}$ mass as well as PAN and $O_3$, which were 156 μg/m$^3$, 2.4 ppbv, and 87.5 ppbv, respectively. Other reactive gases such as CO, $SO_2$, and $NO_2$ were also highly elevated. Note that PAN and $O_3$ gradually increased through the night, leading to a nighttime maximum of both species on November 4th. It is likely that the pre-formed PAN and $O_3$ were continuously transported into Gosan at night.

PAN is formed through the reaction of the peroxyacetyl radical and nitrogen dioxide (Eq. 1) and decomposed at high temperature (Eq. 2), returning these radicals. Unless the NO concentration is high (Eq. 3), the peroxyacetyl radical recombines with $NO_2$, producing PAN. Thus, the total lifetime of PAN depends on the $NO_2$/NO ratio and temperature (Eq. 4) (Brasseur et al., 1999).

$$CH_3C(O)O_2 + NO_2 + M \rightarrow PAN + M \quad (1)$$

$$PAN \rightarrow CH_3C(O)O_2 + NO_2 \quad (2)$$

$$CH_3C(O)O_2 + NO \rightarrow CH_3CO_2 + NO_2 \quad (3)$$

$$T_{eff} = T_d \left(1 + \frac{k_1[NO_2]}{k_2[NO]}\right) \ [sec^{-1}] \quad (4)$$

where $T_d$ and $T_{eff}$ indicate the lifetime against decomposition and the effective lifetime of PAN (Brasseur et al., 1999). The effective lifetime of PAN was estimated through Eq. 4 using the rate constants proposed by Brasseur et al. (1999), Jacobson (2005), and Maricq and Szente (1996).

During the haze event, NO was close to the detection limit, while $NO_2$ was greatly enhanced. Owing to the high $NO_2$/NO ratio, the effective lifetime of PAN increased by 57 ±

14 times; this possibly contributed to the gradual increase in PAN through the night on November 4th. For this estimation, PAN concentration was subtracted from the measured $NO_2$ concentration, considering the positive artifact by molybdenum converter in $NO_2$ measurement. Fischer et al. (2014) also reported that, at night, PAN can be produced from the reaction of acetaldehyde with the nitrate radical.

Besides $PM_{2.5}$ mass, PAN was also well correlated with $PM_{2.5}$ OC and EC not only during this haze episode but also during the entire measurement period (Fig. 6a and b). Furthermore, the enhancement of PAN was concurrent with that of OC and $K^+$, resulting in excellent correlation between them (Fig. 6b and d). In fact, the $\Delta OC/\Delta EC$ ratio of episode 4 was much higher (7) than those of the other episodes (~2.5) (Fig. 6c). The fraction of $PM_{2.5}$ against $PM_{10}$ was also the highest in this episode, indicating significant contribution of secondary aerosols. These observations suggest that air masses were affected by biomass combustion (e.g., Ram et al., 2008, 2012; Saarikoski et al., 2008).

According to previous studies, PAN can be produced in plumes through biomass combustion (Alvarado et al., 2010; Coheur et al., 2007; Liu et al., 2016b; Tereszchuk et al., 2013). In northeast China, open burnings related to agricultural activities frequently occur during the spring and fall (Duan et al., 2004; Yang et al., 2005). Kudo et al. (2014) also reported that, upon burning crop residue in Yangtze region, the levels of oxygenated VOCs were elevated together with $NO_x$. In addition, biofuel is used for cooking and heating and as an energy source in China's industry (Cao et al., 2006).

Therefore, PAN is likely to increase when haze occurs and fine aerosols are transformed as air masses carrying combustion emissions are slowly transported from China over the Yellow Sea. Additionally, the results of this study imply that PAN can be used as a robust tracer for continental outflows in northeast Asia, to identify transport- and chemical transformation-

dominant regimes. In a transport-dominant regime, $O_3$ export was distinguished by the highest levels of primary gaseous species such as $SO_2$ and relatively low levels of PAN. In contrast, fine aerosol species were enhanced in a chemical transformation regime, leading to haze events with relatively more enhanced PAN compared to $O_3$.

Finally, the measured $O_3$ and PAN concentrations were compared to results from a global chemistry model CAM-Chem. In the model simulation, $O_3$ and PAN were highly underestimated during the episodes observed in Chinese outflows, although the variation around average level of $O_3$ and PAN was well captured (Fig. 7). The elevated PAN concentration was underestimated in the model (Oct 20–21 and Nov 4–5), especially when air was impacted by biomass combustion. The timing of the $O_3$ diurnal variability was captured by the model, although the magnitude of the variation was underestimated. These results reveal that the current understanding of Chinese outflow is still not sufficient, thereby causing uncertainty in estimating its effect on air quality in the northwestern Pacific Rim.

## 5. Conclusions

The first measurements of PAN, reactive gases, and aerosol species were conducted at GCO during October 19 to November 6, 2010. The average concentration of PAN was 0.6 ppbv with a maximum of 2.4 ppbv, which was lower than those in major cities in East Asia but much higher than the background concentrations in other regions. Although the hourly concentrations of PAN and $O_3$ were well correlated ($\gamma$ = 0.67), the comparison of the daily maxima of PAN and $O_3$ highlighted that they were not proportionally enhanced. That is, either PAN was relatively more elevated than $O_3$ or the highest $O_3$ was associated with low levels of PAN. Unexpectedly, both PAN and $O_3$ often reached their maxima at night. In this

study, these high concentrations were all encountered in association with continental outflows, where PAN was decoupled from $O_3$ and better correlated with the $PM_{2.5}$ mass ($\gamma = 0.79$) than with $O_3$. Thus, two high-$O_3$ and two high-PAN events were the most clearly distinguished and investigated in detail.

During the $O_3$ episodes, both $O_3$ and PAN concentrations reached their maximum values at night. In episode 1 (Oct. 31 to Nov. 2), the $O_3$ concentration was increased to 80.6 ppbv, with a high $SO_2$ concentration under strong wind. It was a typical Beijing plume observed in the study region. In comparison, $NO_2$ was greatly increased in episode 2 (Oct. 28–29) when the air masses were affected by urban emissions from Korean Peninsula. Although the maximum $O_3$ level was lower during episode 2, these two cases demonstrated well how $O_3$ was exported from the East Asian continent.

The remaining two episodes were highlighted by enhanced PAN concentrations and characterized by haze occurrence. During episode 3 (Oct. 20–21), PAN and $O_3$ concentrations increased up to 2.0 ppbv and 78.9 ppbv, respectively, with high NOx levels, probably influenced by emissions from Korea. Episode 4 (Nov. 4–5) was characterized by the highest concentrations of almost all measured species, including PAN, $O_3$, $PM_{2.5}$ mass, and $PM_{1.0}$ species; the maximum recorded concentrations of PAN, $O_3$, and $PM_{2.5}$ mass during this interval were 2.4 ppbv, 87.5 ppbv, and 156 $\mu g/m^3$, respectively. Note that, along with $PM_{2.5}$ and $O_3$, PAN was gradually increased through the night. In this episode, an air mass was slowly transported from eastern China. With depleted NO, the effective lifetime of PAN was greatly extended. In addition, PAN concentration showed good correlation with OC, EC, and $K^+$; in fact, the correlation of PAN with $K^+$ was comparable to that of OC with $K^+$. These results, in conjunction with the high $\Delta OC/\Delta EC$ (7), imply that the observed haze was mainly caused by the emissions produced by biomass combustion. These results suggest that PAN is

a useful tool for distinguishing continental outflows that were typically observed in northeast Asia.

The comparison between the measured and calculated concentrations using the CAM-Chem-HTAP2 model showed that the model underestimated the $O_3$ and PAN levels in Chinese outflows, particularly for haze incidence. These results reveal that Chinese outflows are still poorly understood and not well captured in the model.

**Acknowledgments**

This study was funded by the Korea Meteorological Administration Research and Development Program under Grant KMIPA 2015-6020. The National Center for Atmospheric Research is funded by the National Science Foundation. The authors gratefully acknowledge the NOAA Air Resources Laboratory (ARL) for the provision of the HYSPLIT transport and dispersion model and/or READY website (http://www.ready.noaa.gov) used in this publication.

## References


Akimoto, H.: Global air quality and pollution, Science, 302, 1716-1719, doi:10.1126/science.1092666, 2003.

Alvarado, M. J., Logan, J. A., Mao, J., Apel, E., Riemer, D., Blake, D., Cohen, R. C., Min, K. E., Perring, A. E., Browne, E. C., Wooldridge, P. J., Diskin, G. S., Sachse, G. W., Fuelberg, H., Sessions, W. R., Harrigan, D. L., Huey, G., Liao, J., Case-Hanks, A., Jimenez, J. L., Cubison, M. J., Vay, S. A., Weinheimer, A. J., Knapp, D. J., Montzka, D. D., Flocke, F. M., Pollack, I. B., Wennberg, P. O., Kurten, A., Crounse, J., Clair, J. M. S., Wisthaler, A., Mikoviny, T., Yantosca, R. M., Carouge, C. C., and Le Sager, P.: Nitrogen oxides and PAN in plumes from boreal fires during ARCTAS-B and their impact on ozone: an integrated analysis of aircraft and satellite observations, Atmos. Chem. Phys., 10, 9739-9760, doi:10.5194/acp-10-9739-2010, 2010.

Aneja, V. P., Hartsell, B. E., Kim, D. S., and Grosjean, D.: Peroxyacetyl nitrate in Atlanta, Georgia: Comparison and analysis of ambient data for suburban and downtown locations, J. Air & Waste Manage. Assoc., 49, doi: 177-184, 10.1080/10473289.1999.10463786, 1999.

Banta, R. M., Senff, C. J., White, A. B., Trainer, M., McNider, R. T., Valente, R. J., Mayor, S. D., Alvarez, R. J., Hardesty, R. M., Parrish, D., and Fehsenfeld, F. C.: Daytime buildup and nighttime transport of urban ozone in the boundary layer during a stagnation episode, J. Geophys. Res. Atmos., 103, 22519-22544, doi:10.1029/98jd01020, 1998.

Beine, H. J., Jaffe, D. A., Herring, J. A., Kelley, J. A., Krognes, T., and Stordal, F.: High-latitude springtime photochemistry .1. NOx, PAN and ozone relationships, J. Atmos. Chem., 27, 127-153, doi:10.1023/a:1005869900567, 1997.

Bertram, T. H., Perring, A. E., Wooldridge, P. J., Dibb, J., Avery, M. A., and Cohen, R. C.: On the export of reactive nitrogen from Asia: $NO_x$ partitioning and effects on ozone, Atmos. Chem. Phys., 13, 4617-4630, doi:10.5194/acp-13-4617-2013, 2013.

Brasseur, G. P., Orlando, J. J., and Tyndall, G. S.: Atmospheric chemistry and global change, Oxford University Press, New York, 235-347 pp., 1999.

Cao, G., Zhang, X., and Zheng, F.: Inventory of black carbon and organic carbon emissions from China, Atmos. Environ., 40, 6516-6527, doi:10.1016/j.atmosenv.2006.05.070, 2006.

Coheur, P. F., Herbin, H., Clerbaux, C., Hurtmans, D., Wespes, C., Carleer, M., Turquety, S., Rinsland, C. P., Remedios, J., Hauglustaine, D., Boone, C. D., and Bernath, P. F.: ACE-FTS observation of a young biomass burning plume: first reported measurements of $C_2H_4$, $C_3H_6O$, $H_2CO$ and PAN by infrared occultation from space, Atmos. Chem. Phys., 7, 5437-5446, doi:10.5194/acp-7-5437-2007, 2007.

Draxler, R. R., and Rolph, G. D.: HYSPLIT (HYbrid Single-Particle Lagrangian Integrated Trajectory) Model access via NOAA ARL READY Website (http://ready.arl.noaa.gov/HYSPLIT.php), NOAA Air Resources Laboratory, Silver Spring, MD., 2012.

Duan, F., Liu, X., Yu, T., and Cachier, H.: Identification and estimate of biomass burning contribution to the urban aerosol organic carbon concentrations in Beijing, Atmos. Environ., 38, 1275-1282, doi:10.1016/j.atmosenv.2003.11.037, 2004.

417 Fischer, E. V., Jaffe, D. A., Reidmiller, D. R., and Jaeglé, L.: Meteorological controls on
418 observed peroxyacetyl nitrate at Mount Bachelor during the spring of 2008, J. Geophys.
419 Res., 115, D03302, doi:10.1029/2009jd012776, 2010.

420 Fischer, E. V., Jaffe, D. A., and Weatherhead, E. C.: Free tropospheric peroxyacetyl nitrate
421 (PAN) and ozone at Mount Bachelor: potential causes of variability and timescale for
422 trend detection, Atmos. Chem. Phys., 11, 5641-5654, doi:10.5194/acp-11-5641-2011,
423 2011.

424 Fischer, E. V., Jacob, D. J., Yantosca, R. M., Sulprizio, M. P., Millet, D. B., Mao, J., Paulot, F.,
425 Singh, H. B., Roiger, A., Ries, L., Talbot, R. W., Dzepina, K., and Pandey, D. S.:
426 Atmospheric peroxyacetyl nitrate (PAN): a global budget and source attribution, Atmos.
427 Chem. Phys., 14, 2679-2698, doi:10.5194/acp-14-2679-2014, 2014.

428 Gaffney, J. S., Fajer, R., and Senum, G. I.: An improved procedure for high purity gaseous
429 peroxyacyl nitrate production: Use of heavy lipid solvents, Atmos. Environ., 18, 215-
430 218, doi:10.1016/0004-6981(84)90245-2, 1984.

431 Gaffney, J. S., Bornick, R. M., Chen, Y. H., and Marley, N. A.: Capillary gas chromatographic
432 analysis of nitrogen dioxide and pans with luminol chemiluminescent detection, Atmos.
433 Environ., 32, 1445-1454, doi:10.1016/S1352-2310(97)00098-8, 1998.

434 Gaffney, J. S., Marley, N. A., Cunningham, M. M., and Doskey, P. V.: Measurements of
435 peroxyacyl nitrates (PANs) in Mexico City: implications for megacity air quality
436 impacts on regional scales, Atmos. Environ., 33, 5003-5012, doi:10.1016/S1352-
437 2310(99)00263-0, 1999.

438 Gallagher, M. S., Carsey, T. P., and Farmer, M. L.: Peroxyacetyl nitrate in the North Atlantic
439 marine boundary layer, Global Biogeochem. Cycle., 4, 297-308,
440 doi:10.1029/GB004i003p00297, 1990.

441 Gregory, G. L.: An intercomparison of airborne PAN measurements, J. Geophys. Res., 95,
442 10077-10087, doi:10.1029/JD095iD07p10077, 1990.

443 Grosjean, E., Grosjean, D., Woodhouse, L. F., and Yang, Y.-J.: Peroxyacetyl nitrate and
444 peroxypropionyl nitrate in Porto Alegre, Brazil, Atmos. Environ., 36, 2405-2419,
445 doi:10.1016/S1352-2310(01)00541-6, 2002.

446 Gu, D., Wang, Y., Smeltzer, C., and Liu, Z.: Reduction in NOx Emission Trends over China:
447 Regional and Seasonal Variations, Environ. Sci. Technol., 47, 12912–12919,
448 doi:10.1021/es401727e, 2013.

449 Hansel, A., and Wisthaler, A.: A method for real-time detection of PAN, PPN and MPAN in
450 ambient air, Geophys. Res. Lett., 27, 895-898, doi:10.1029/1999gl010989, 2000.

451 Jacob, D. J.: Introduction to atmospheric chemistry, 199-231 pp., 1999.

452 Jacob, D. J.: Heterogeneous chemistry and tropospheric ozone, Atmos. Environ., 34, 2131-
453 2159, doi:10.1016/s1352-2310(99)00462-8, 2000.

454 Jacobson, M. Z.: Fundamentals of atmospheric modeling, Second edition, Cambridge, UK,
455 731-738 pp., 2005.

456 Jaffe, D. A., Thornton, J., Wolfe, G., Reidmiller, D., Fischer, E. V., Jacob, D. J., Zhang, L.,
457 Cohen, R., Singh, H., Weinheimer, A., and Flocke, F.: Can we detect an Influence over
458 North America from Increasing Asian NOx Emissions?, Eos Trans, AGU, 88, 2007.

Janssens-Maenhout, G., Crippa, M., Guizzardi, D., Dentener, F., Muntean, M., Pouliot, G., Keating, T., Zhang, Q., Kurokawa, J., Wankmüller, R., Denier van der Gon, H., Kuenen, J. J. P., Klimont, Z., Frost, G., Darras, S., Koffi, B., and Li, M.: HTAP_v2.2: a mosaic of regional and global emission grid maps for 2008 and 2010 to study hemispheric transport of air pollution, Atmos. Chem. Phys., 15, 11411-11432, doi:10.5194/acp-15-11411-2015, 2015.

Kanaya, Y., Tanimoto, H., Matsumoto, J., Furutani, H., Hashimoto, S., Komazaki, Y., Tanaka, S., Yokouchi, Y., Kato, S., Kajii, Y., and Akimoto, H.: Diurnal variations in $H_2O_2$, $O_3$, PAN, $HNO_3$ and aldehyde concentrations and $NO/NO_2$ ratios at Rishiri Island, Japan: Potential influence from iodine chemistry, Sci. Total Envir., 376, 185-197, doi:10.1016/j.scitotenv.2007.01.073, 2007.

Kenley, R. A., and Hendry, D. G.: Generation of peroxy radicals from peroxynitrates ($ROONO_2$). Decomposition of peroxybenzoyl nitrate (PBzN), J. Am. Chem. Soc., 104, 220-224, doi:10.1021/ja00365a040, 1982.

Kourtidis, K. A., Fabian, P., Zerefos, C., and RappenglÜCk, B.: Peroxyacetyl nitrate (PAN), peroxypropionyl nitrate (PPN) and PAN/ozone ratio measurements at three sites in Germany, Tellus B, 45, 442-457, doi:10.1034/j.1600-0889.1993.t01-3-00004.x, 1993.

Krotkov, N. A., McLinden, C. A., Li, C., Lamsal, L. N., Celarier, E. A., Marchenko, S. V., Swartz, W. H., Bucsela, E. J., Joiner, J., Duncan, B. N., Boersma, K. F., Veefkind, J. P., Levelt, P. F., Fioletov, V. E., Dickerson, R. R., He, H., Lu, Z., and Streets, D. G.: Aura OMI observations of regional SO2 and NO2 pollution changes from 2005 to 2015, Atmos. Chem. Phys., 16, 4605–4629, doi:10.5194/acp-16-4605-2016, 2016.

Kudo, S., Tanimoto, H., Inomata, S., Saito, S., Pan, X., Kanaya, Y., Taketani, F., Wang, Z., Chen, H., Dong, H., Zhang, M., and Yamaji, K.: Emissions of nonmethane volatile organic compounds from open crop residue burning in the Yangtze River Delta region, China, J. Geophys. Res., 119, 7684–7698, doi:10.1002/2013JD021044, 2014.

LaFranchi, B. W., Wolfe, G. M., Thornton, J. A., Harrold, S. A., Browne, E. C., Min, K. E., Wooldridge, P. J., Gilman, J. B., Kuster, W. C., Goldan, P. D., De Gouw, J. A., McKay, M., Goldstein, A. H., Ren, X., Mao, J., and Cohen, R. C.: Closing the peroxy acetyl nitrate budget: Observations of acyl peroxy nitrates (PAN, PPN, and MPAN) during BEARPEX 2007, Atmos. Chem. Phys., 9, 7623-7641, doi:10.5194/acp-9-7623-2009, 2009.

Lamarque, J. F., Emmons, L. K., Hess, P. G., Kinnison, D. E., Tilmes, S., Vitt, F., Heald, C. L., Holland, E. A., Lauritzen, P. H., Neu, J., Orlando, J. J., Rasch, P. J., and Tyndall, G. K.: CAM-chem: description and evaluation of interactive atmospheric chemistry in the Community Earth System Model, Geosci. Model Dev., 5, 369-411, doi:10.5194/gmd-5-369-2012, 2012.

Lee, G., Jang, Y., Lee, H., Han, J.-S., Kim, K.-R., and Lee, M.: Characteristic behavior of peroxyacetyl nitrate (PAN) in Seoul megacity, Korea, Chemosphere, 73, 619-628, doi:10.1016/j.chemosphere.2008.05.060, 2008.

Lee, G., Choi, H.-S., Lee, T., Choi, J., Park, J. S., and Ahn, J. Y.: Variations of regional background peroxyacetyl nitrate in marine boundary layer over Baengyeong Island, South Korea, Atmos. Environ., 61, 533-541, doi:10.1016/j.atmosenv.2012.07.075, 2012.

Lee, M., Song, M., Moon, K. J., Han, J. S., Lee, G., and Kim, K.-R.: Origins and chemical

503 characteristics of fine aerosols during the northeastern Asia regional experiment
504 (Atmospheric Brown Cloud-East Asia Regional Experiment 2005), J. Geophys. Res.,
505 112, D22S29, doi:10.1029/2006jd008210, 2007.

506 Li, M., Zhang, Q., Kurokawa, J., Woo, J. H., He, K. B., Lu, Z., Ohara, T., Song, Y., Streets, D.
507 G., Carmichael, G. R., Cheng, Y. F., Hong, C. P., Huo, H., Jiang, X. J., Kang, S. C., Liu,
508 F., Su, H., and Zheng, B.: MIX: a mosaic Asian anthropogenic emission inventory for
509 the MICS-Asia and the HTAP projects, Atmos. Chem. Phys. Discuss., 2015, 34813-
510 34869, doi:10.5194/acpd-15-34813-2015, 2015.

511 Lim, S., Lee, M., Lee, G., Kim, S., Yoon, S., and Kang, K.: Ionic and carbonaceous
512 compositions of $PM_{10}$, $PM_{2.5}$ and $PM_{1.0}$ at Gosan ABC Superstation and their ratios as
513 source signature, Atmos. Chem. Phys., 12, 2007-2024, doi:10.5194/acp-12-2007-2012,
514 2012.

515 Liu, F., Zhang, Q., A., van der A, R. J., Zheng, B., Tong, D., Yan, L., Zheng, Y., and He, K.:
516 Recent reduction in NO x emissions over China: synthesis of satellite observations and
517 emission inventories, Environmental Research Letters, 11, 114002, doi:10.1088/1748-
518 9326/11/11/114002, 2016a.

519 Liu, Z., Wang, Y., Gu, D., Zhao, C., Huey, L. G., Stickel, R., Liao, J., Shao, M., Zhu, T., Zeng,
520 L., Liu, S.-C., Chang, C.-C., Amoroso, A., and Costabile, F.: Evidence of reactive
521 aromatics as a major source of peroxy acetyl nitrate over China, Environ. Sci. Technol.,
522 44, 7017-7022, doi:10.1021/es1007966, 2010.

523 Liu, X., Zhang, Y., Huey, L. G., Yokelson, R. J., Wang, Y., Jimenez, J. L., Campuzano-Jost, P.,
524 Beyersdorf, A. J., Blake, D. R., Choi, Y., St. Clair, J. M., Crounse, J. D., Day, D. A.,
525 Diskin, G. S., Fried, A., Hall, S. R., Hanisco, T. F., King, L. E., Meinardi, S., Mikoviny,
526 T., Palm, B. B., Peischl, J., Perring, A. E., Pollack, I. B., Ryerson, T. B., Sachse, G.,
527 Schwarz, J. P., Simpson, I. J., Tanner, D. J., Thornhill, K. L., Ullmann, K., Weber, R. J.,
528 Wennberg, P. O., Wisthaler, A., Wolfe, G. M., and Ziemba, L. D.: Agricultural fires in
529 the southeastern U.S. during SEAC4RS: Emissions of trace gases and particles and
530 evolution of ozone, reactive nitrogen, and organic aerosol, J. Geophys, Res.- Atmos.,
531 121, 7383-7414, doi:10.1002/2016JD025040, 2016b.

532 Maricq, M. M., and Szente, J. J.: Temperature-dependent study of the $CH_3C(O)O_2$ + NO
533 reaction, J. Phys. Chem., 100, 12380-12385, doi:10.1021/jp960792c, 1996.

534 Marley, N. A., Gaffney, J. S., White, R. V., Rodriguez-Cuadra, L., Herndon, S. E., Dunlea, E.,
535 Volkamer, R. M., Molina, L. T., and Molina, M. J.: Fast gas chromatography with
536 luminol chemiluminescence detection for the simultaneous determination of nitrogen
537 dioxide and peroxyacetyl nitrate in the atmosphere, Rev. Sci. Instr., 75, 4595-4605,
538 doi:10.1063/1.1805271, 2004.

539 Mills, G. P., Sturges, W. T., Salmon, R. A., Bauguitte, S. J. B., Read, K. A., and Bandy, B. J.:
540 Seasonal variation of peroxyacetylnitrate (PAN) in coastal Antarctica measured with a
541 new instrument for the detection of sub-part per trillion mixing ratios of PAN, Atmos.
542 Chem. Phys., 7, 4589-4599, doi:10.5194/acp-7-4589-2007, 2007.

543 Muller, K. P., and Rudolph, J.: Measurements of peroxyacetylnitrate in the marine boundary
544 layer over the Atlantic, J. Atmos. Chem., 15, 361-367, doi:10.1007/BF00115405, 1992.

545 Nielsen, T., Samuelsson, U., Grennfelt, P., and Thomsen, E. L.: Peroxyacetyl nitrate in long-
546 range transported polluted air, Nature, 293, 553-555, doi:10.1038/293553a0, 1981.

NIER, Annual Report of Ambient Air Quality in Korea, 2015, National Institute of Environmental Research, Inchon, Korea, 350pp., 2016a (in Korean).

NIER, Guidelines for installation and operation of air pollution monitoring network, National Institute of Environmental Research, Inchon, Korea, 427 pp., 2016b (in Korean).

Ohara, T., Akimoto, H., Kurokawa, J., Horii, N., Yamaji, K., Yan, X., and Hayasaka, T.: An Asian emission inventory of anthropogenic emission sources for the period 1980-2020, Atmos. Chem. Phys., 7, 4419-4444, doi:10.5194/acp-7-4419-2007, 2007.

Ram, K., Sarin, M. M., and Hegde, P.: Atmospheric abundances of primary and secondary carbonaceous species at two high-altitude sites in India: Sources and temporal variability, Atmos. Environ., 42, 6785-6796, doi:10.1016/j.atmosenv.2008.05.031, 2008.

Ram, K., Sarin, M. M., and Tripathi, S. N.: Temporal trends in atmospheric $PM_{2.5}$, $PM_{10}$, elemental carbon, organic carbon, water-soluble organic carbon, and optical properties: Impact of biomass burning emissions in the Indo-Gangetic Plain, Environ. Sci. Technol., 46, 686-695, doi:10.1021/es202857w, 2012.

Randerson, J. T., van der Werf, G. R., Giglio, L., Collatz, G. J., and Kasibhatla, P. S.: Global Fire Emissions Database, Version 3 (GFEDv3.1). Data set. Available on-line [http://daac.ornl.gov/] from Oak Ridge National Laboratory Distributed Active Archive Center, Oak Ridge, Tennessee, USA. doi:10.3334/ORNLDAAC/1191, 2013.

Ridley, B. A., Shetter, J. D., Gandrud, B. W., Salas, L. J., Singh, H. B., Carroll, M. A., Hubler, G., Albritton, D. L., Hastie, D. R., Schiff, H. I., Mackay, G. I., Karechi, D. R., Davis, D. D., Bradshaw, J. D., Rodgers, M. O., Sandholm, S. T., Torres, A. L., Condon, E. P., Gregory, G. L., and Beck, S. M.: Ratios of peroxyacetyl nitrate to active nitrogen observed during aircraft flights over the Eastern Pacific Oceans and continental United-States, J. Geophys. Res., 95, 10179-10192, doi:10.1029/JD095iD07p10179, 1990.

Roberts, J. M., Flocke, F., Chen, G., de Gouw, J., Holloway, J. S., Hübler, G., Neuman, J. A., Nicks, D. K., Nowak, J. B., Parrish, D. D., Ryerson, T. B., Sueper, D. T., Warneke, C., and Fehsenfeld, F. C.: Measurement of peroxycarboxylic nitric anhydrides (PANs) during the ITCT 2K2 aircraft intensive experiment, J. Geophys, Res.- Atmos., 109, D23S21, doi:10.1029/2004JD004960, 2004.

Roberts, J. M., Marchewka, M., Bertman, S. B., Sommariva, R., Warneke, C., de Gouw, J., Kuster, W., Goldan, P., Williams, E., Lerner, B. M., Murphy, P., and Fehsenfeld, F. C.: Measurements of PANs during the New England Air Quality Study 2002, J. Geophys. Res., 112, D20306, doi:10.1029/2007JD008667, 2007.

Rolph, G. D.: Real-time Environmental Applications and Display sYstem (READY) Website (http://ready.arl.noaa.gov). NOAA Air Resources Laboratory, Silver Spring, MD. , 2012.

Saarikoski, S., Timonen, H., Saarnio, K., Aurela, M., Ĵrvi, L., Keronen, P., Kerminen, V. M., and Hillamo, R.: Sources of organic carbon in fine particulate matter in northern European urban air, Atmos. Chem. Phys., 8, 6281-6295, doi:10.5194/acp-8-6281-2008, 2008.

Schrimpf, W., Muller, K. P., Johnen, F. J., Lienaerts, K., and Rudolph, J.: An optimized method for airborne peroxyacetyl nitrate (PAN) measurements, J. Atmos. Chem., 22, 303-317, doi:10.1007/bf00696640, 1995.

Shang, X., Lee, M., Han, J., Kang, E., Gustafsson, Ö., and Chang, L.-S.: Identifiction and

590 chemical characteristics of distinctive Chinese outflow plumes associated with enhanced
591 submicron aerosols at Gosan Climate Observatory, submitted at Aerosol Air Qual. Res.

592 Staudt, A. C., Jacob, D. J., Ravetta, F., Logan, J. A., Bachiochi, D., Sandholm, S., Ridley, B.,
593 Singh, H. B., and Talbot, B.: Sources and chemistry of nitrogen oxides over the tropical
594 Pacific, J. Geophys. Res., 108, 8239, doi:10.1029/2002JD002139, 2003.

595 Stjern, C. W., Samset, B. H., Myhre, G., Bian, H., Chin, M., Davila, Y., Dentener, F.,
596 Emmons, L., Flemming, J., Haslerud, A. S., Henze, D., Jonson, J. E., Kucsera, T., Lund,
597 M. T., Schulz, M., Sudo, K., Takemura, T., and Tilmes, S.: Global and regional radiative
598 forcing from 20% reductions in BC, OC and SO4 – an HTAP2 multi-model study,
599 Atmos. Chem. Phys., 16, 13579-13599, doi:10.5194/acp-16-13579-2016, 2016.

600 Talukdar, R. K., Burkholder, J. B., Schmoltner, A. M., Roberts, J. M., Wilson, R. R., and
601 Ravishankara, A. R.: Investigation of the loss processes for peroxyacetyl nitrate in the
602 atmosphere: UV photolysis and reaction with OH, J. Geophys. Res., 100, 14163-14173,
603 doi:10.1029/95JD00545, 1995.

604 Tanimoto, H., Hirokawa, J., Kajii, Y., and Akimoto, H.: A new measurement technique of
605 peroxyacetyl nitrate at parts per trillion by volume levels: Gas chromatography/negative
606 ion chemical ionization mass spectrometry, J. Geophys. Res., 104(17), 21, 343-21, 354,
607 doi:10.1029/1999JD900345, 1999.

608 Tanimoto, H., H. Furutani, S. Kato, J. Matsumoto, Y. Makide, and H. Akimoto, Seasonal
609 cycles of ozone and oxidized nitrogen species in northeast Asia, 1, Impact of regional
610 climatology and photochemistry observed during RISOTTO 1999-2000, J. Geophys.
611 Res., 107(D24), 4747, doi:10.1029/2001JD001496, 2002.

612 Tanimoto, H., K. Matsumoto, and M. Uematsu, Ozone–CO correlations in Siberian wildfire
613 plumes observed at Rishiri Island, SOLA, 4, 65-68, doi:10.2151/sola.2008-017, 2008.

614 Tereszchuk, K. A., Moore, D. P., Harrison, J. J., Boone, C. D., Park, M., Remedios, J. J.,
615 Randel, W. J., and Bernath, P. F.: Observations of peroxyacetyl nitrate (PAN) in the
616 upper troposphere by the Atmospheric Chemistry Experiment-Fourier Transform
617 Spectrometer (ACE-FTS), Atmos. Chem. Phys., 13, 5601-5613, doi:10.5194/acp-13-
618 5601-2013, 2013.

619 Tilmes, S., Lamarque, J. F., Emmons, L. K., Kinnison, D. E., Ma, P. L., Liu, X., Ghan, S.,
620 Bardeen, C., Arnold, S., Deeter, M., Vitt, F., Ryerson, T., Elkins, J. W., Moore, F.,
621 Spackman, J. R., and Val Martin, M.: Description and evaluation of tropospheric
622 chemistry and aerosols in the Community Earth System Model (CESM1.2), Geosci.
623 Model Dev., 8, 1395-1426, doi:10.5194/gmd-8-1395-2015, 2015.

624 Villena, G., Bejan, I., Kurtenbach, R., Wiesen, P., and Kleffmann, J.: Interferences of
625 commercial $NO_2$ instruments in the urban atmosphere and in a smog chamber, Atmos.
626 Meas. Tech., 5, 149-159, dio:10.5194/amt-5-149-2012, 2012.

627 Wang, B., Shao, M., Roberts, J. M., Yang, G., Yang, F., Hu, M., Zeng, L., Zhang, Y., and
628 Zhang, J.: Ground-based on-line measurements of peroxyacetyl nitrate (PAN) and
629 peroxypropionyl nitrate (PPN) in the Pearl River Delta, China, Int. J. Environ. Anal.
630 Chem., 90, 548-559, doi:10.1080/03067310903194972, 2010.

631 Wang, Y., Zhang, Y., Hao, J., and Luo, M.: Seasonal and spatial variability of surface ozone
632 over China: contributions from background and domestic pollution, Atmos. Chem. Phys.,

11, 3511-3525, doi:10.5194/acp-11-3511-2011, 2011.

Yang, F., He, K., Ye, B., Chen, X., Cha, L., Cadle, S. H., Chan, T., and Mulawa, P. A.: One-year record of organic and elemental carbon in fine particles in downtown Beijing and Shanghai, Atmos. Chem. Phys., 5, 1449-1457, doi:10.5194/acp-5-1449-2005, 2005.

Zhang, H., Xu, X., Lin, W., and Wang, Y.: Wintertime peroxyacetyl nitrate (PAN) in the megacity Beijing: Role of photochemical and meteorological processes, J. Environ. Sci., 26, 83-96, doi:10.1016/S1001-0742(13)60384-8, 2014.

Zhang, J. B., Xu, Z., Yang, G., and Wang, B.: Peroxyacetyl nitrate (PAN) and peroxypropionyl nitrate (PPN) in urban and suburban atmospheres of Beijing, China, Atmos. Chem. Phys. Discuss., 11, 8173-8206, doi:10.5194/acpd-11-8173-2011, 2011.

Zhang, J. M., Wang, T., Ding, A. J., Zhou, X. H., Xue, L. K., Poon, C. N., Wu, W. S., Gao, J., Zuo, H. C., Chen, J. M., Zhang, X. C., and Fan, S. J.: Continuous measurement of peroxyacetyl nitrate (PAN) in suburban and remote areas of western China, Atmos. Environ., 43, 228-237, doi:10.1016/j.atmosenv.2008.09.070, 2009.

Zhang, L., Jacob, D. J., Boersma, K. F., Jaffe, D. A., Olson, J. R., Bowman, K. W., Worden, J. R., Thompson, A. M., Avery, M. A., Cohen, R. C., Dibb, J. E., Flock, F. M., Fuelberg, H. E., Huey, L. G., McMillan, W. W., Singh, H. B., and Weinheimer, A. J.: Transpacific transport of ozone pollution and the effect of recent Asian emission increases on air quality in North America: An integrated analysis using satellite, aircraft, ozonesonde, and surface observations, Atmos. Chem. Phys., 8, 6117-6136, doi:10.5194/acp-8-6117-2008, 2008.

Zhao, B., Wang, S. X., Liu, H., Xu, J. Y., Fu, K., Klimont, Z., Hao, J. M., He, K. B., Cofala, J., and Amann, M.: NOx emissions in China: historical trends and future perspectives, Atmos. Chem. Phys., 13, 9869–9897, doi:10.5194/acp-13-9869-2013, 2013.

Zhu, L., Fischer, E. V., Payne, V. H., Worden, J. R., and Jiang, Z.: TES observations of the interannual variability of PAN over Northern Eurasia and the relationship to springtime fires, Geophys. Res. Lett., 42, 7230-7237, dio:10.1002/2015GL065328, 2015.

Zhu, L., Payne, V. H., Walker, T. W., Worden, J. R., Jiang, Z., Kulawik, S. S., and Fischer, E. V.: PAN in the eastern Pacific free troposphere: A satellite view of the sources, seasonality, interannual variability, and timeline for trend detection, J. Geophys, Res.-Atmos., 122, 3614-3629, doi:10.1002/2016JD025868, 2017.

664 **Tables**

665

666 Table 1. Chemical and meteorological characteristics of the four episodes.

| | Episode 1 | Episode 2 | Episode 3 | Episode 4 |
|---|---|---|---|---|
| Period | Oct.31 ~ Nov.2 | Oct. 28~29 | Oct. 20~21 | Nov. 4~5 |
| Type | Transport dominant | Transport dominant | Chemical transformation | Chemical transformation |
| Event | $O_3$ export | $O_3$ export | Haze | Haze |
| $O_3$ (ppbv) | 60.2 (80.6) | 45.6 (62.8) | 59.7 (78.9) | 61.8 (87.5) |
| PAN (ppbv) | 0.5 (0.9) | 0.5 (0.8) | 1.2 (2.0) | 1.3 (2.4) |
| $PM_{2.5}$ ($\mu g/m^3$) | 34 (62) | 23 (36) | 50 (76) | 77 (156) |
| $SO_2$ (ppbv) | 4.3 (12.9) | 2.0 (4.4) | 2.6 (5.4) | 4.4 (9.5) |
| $NO_2$ (ppbv) | 3.7 (7.3) | 6.2 (12.1) | 6.2 (12.7) | 6.1 (9.9) |
| Wind Speed (m/s) | 13.5 (16.0) | 9.5 (16.1) | 6.6 (10.2) | 5.0 (7.7) |

667 *Measurements are given for the average with the maximum in the parenthesis.

668 **Figure Captions**

669

670 Figure 1. Temporal variations (against local time) of measured species, including PAN, $PM_{2.5}$,
671 $O_3$, $NO_2$, NO, $SO_2$, and, CO, and meteorological parameters, including relative
672 humidity, temperature, and wind speed in fall 2010. Episodes 1–4, described in the
673 main text, are shaded in blue and yellow.

674 Figure 2. Diurnal variations in the concentrations of $O_3$, $NO_2$, PAN, and $PM_{2.5}$, measured at
675 GCO in the fall of 2010 (5 min data of $O_3$, $NO_2$, 2 min data of PAN, and 1 h data of
676 $PM_{2.5}$).

677 Figure 3. Comparison of $O_3$ with the PAN daily maxima. The time when the daily maximum
678 appears is classified as daytime (08–18 h) and nighttime (the rest) based on the
679 time of sunrise and sunset. Numerals indicate the days.

680 Figure 4. The three-day NOAA HYSPLIT backward trajectories of air masses for every one
681 hour observed at GCO during episode 1 (Oct. 31to Nov. 2), episode 2 (Oct. 28–29),
682 episode 3 (Oct. 20–21), and episode 4 (Nov. 4–5). They are colored according to
683 the level of (a) PAN, (b) $O_3$, (c) $NO_2$, and (d) $PM_{2.5}$ at GCO at the time of the
684 trajectory initialization. The trajectories north of 50°N are not shown. For these
685 horizontal trajectories, (e) vertical heights are given.

686 Figure 5. Correlations between (a) PAN and $O_3$ and (b) PAN and $NO_2$ with linear regression
687 line for each episode. Correlations between $O_3$ and PAN were color coded by the
688 level of (c) $NO_2$ and (d) $PM_{2.5}$.

689 Figure 6. Correlations among PAN, $K^+$ ion of $PM_{1.0}$, and carbonaceous components of $PM_{2.5}$
690 for three cases: (a) PAN and $PM_{2.5}$ mass, (b) PAN and $PM_{2.5}$ OC, (d) $PM_{2.5}$ EC and
691 OC, and (d) PAN and $PM_{1.0}$ $K^+$. The lines represent the linear regression for each
692 episode.

693 Figure 7. Comparison between the observed and calculated (a) PAN and (b) $O_3$
694 concentrations by CAM-chem model. Time is given in local time and four episodes
695 are shaded.

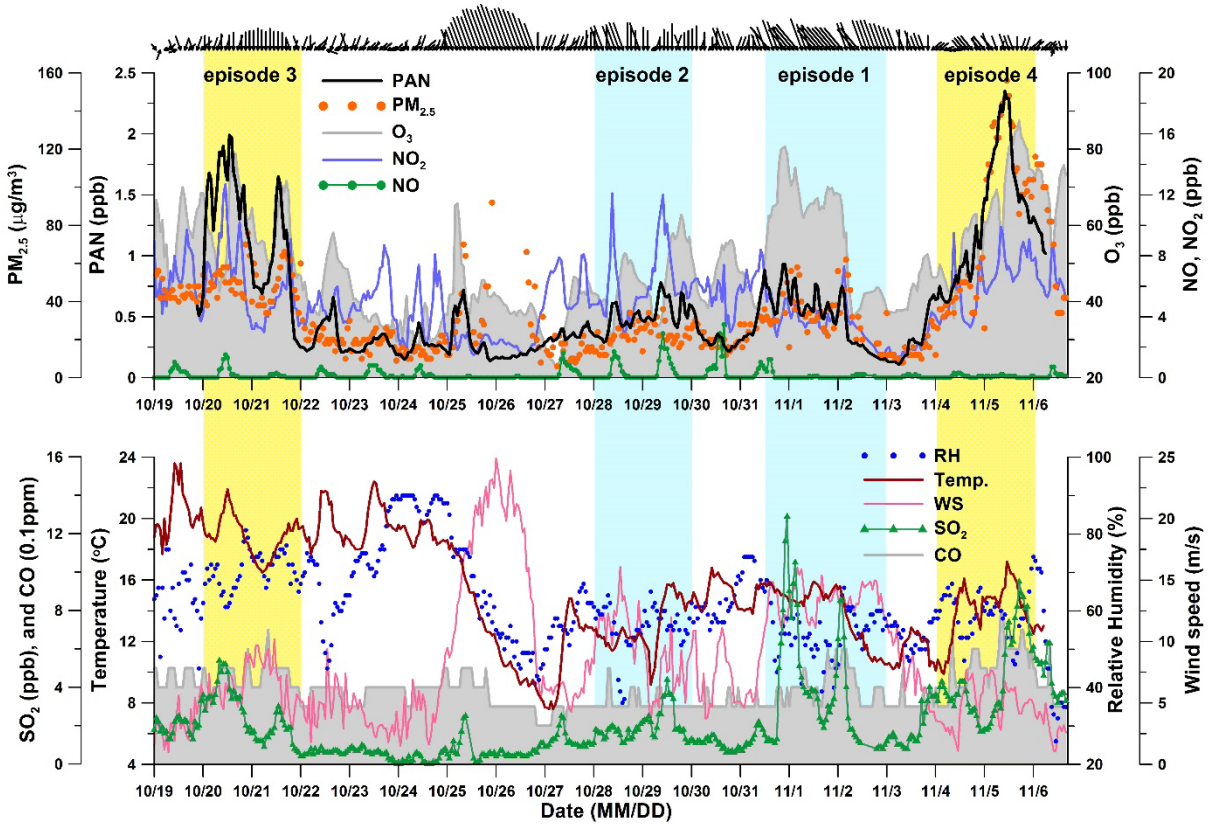


696

697 Figure 1.

698

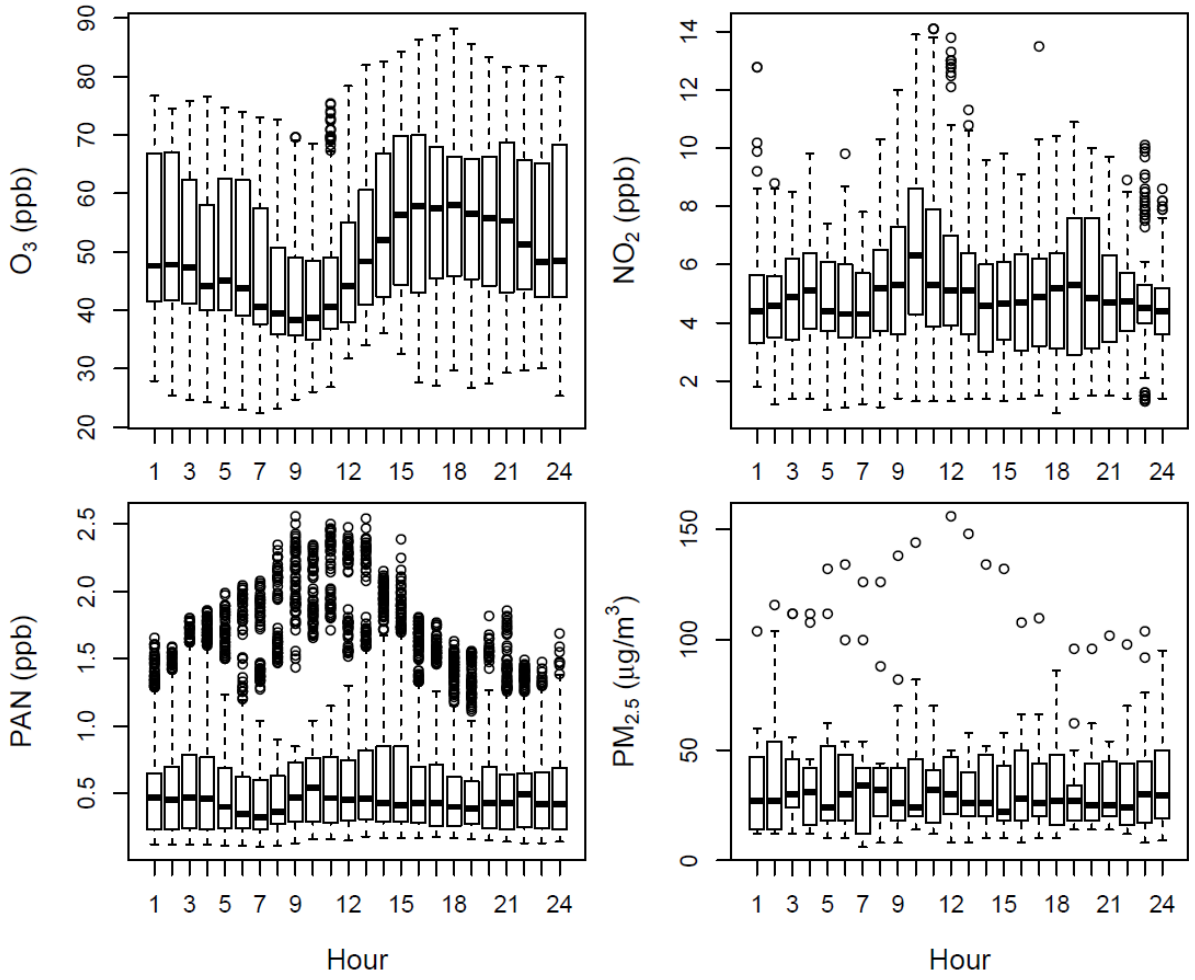


699

700 Figure 2.

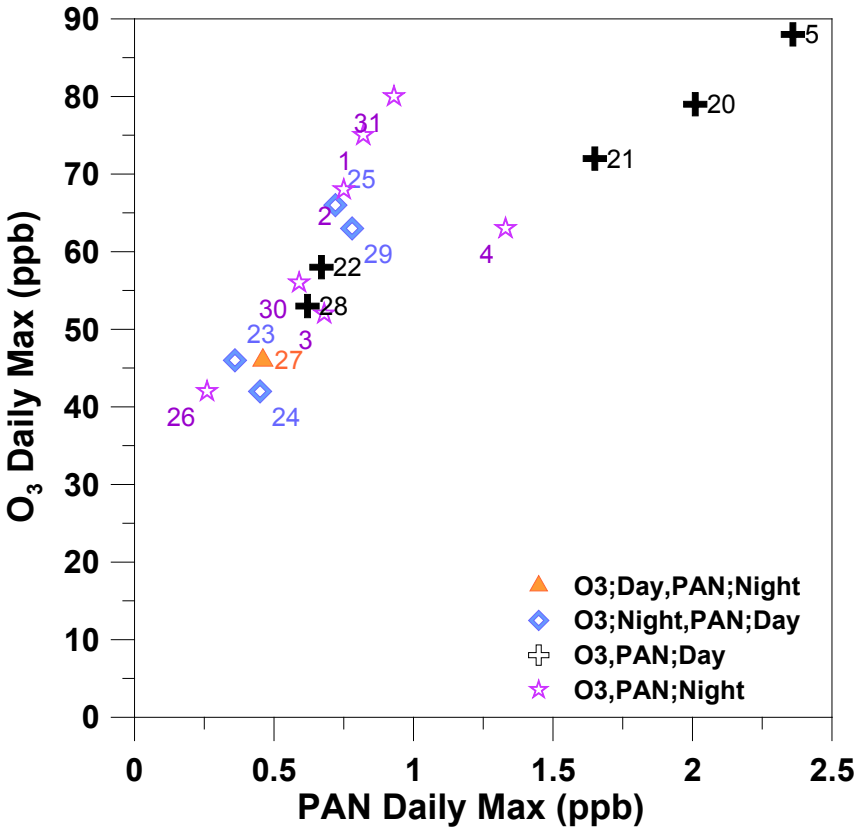


701

702 Figure 3.

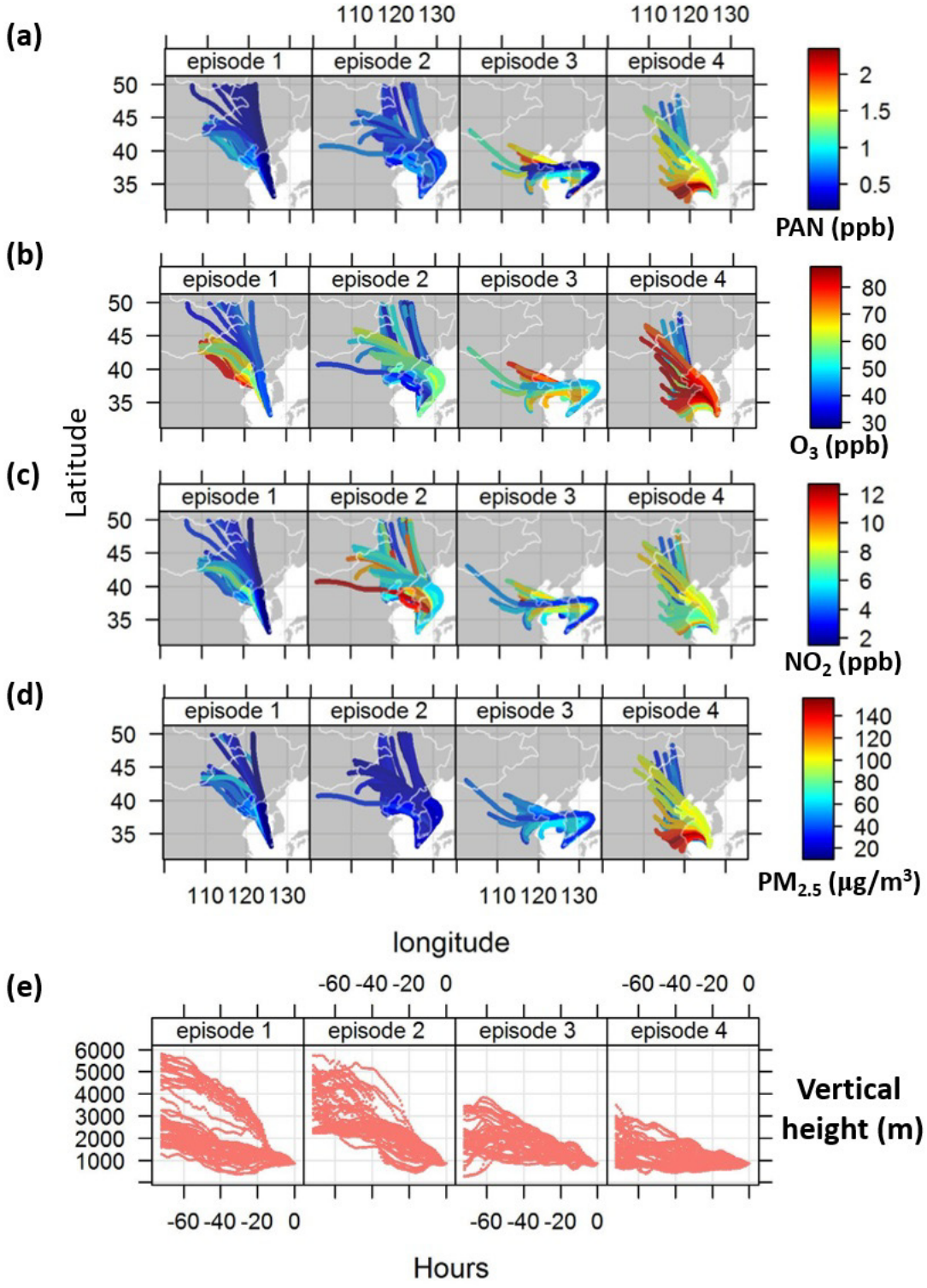


703

704 Figure 4.

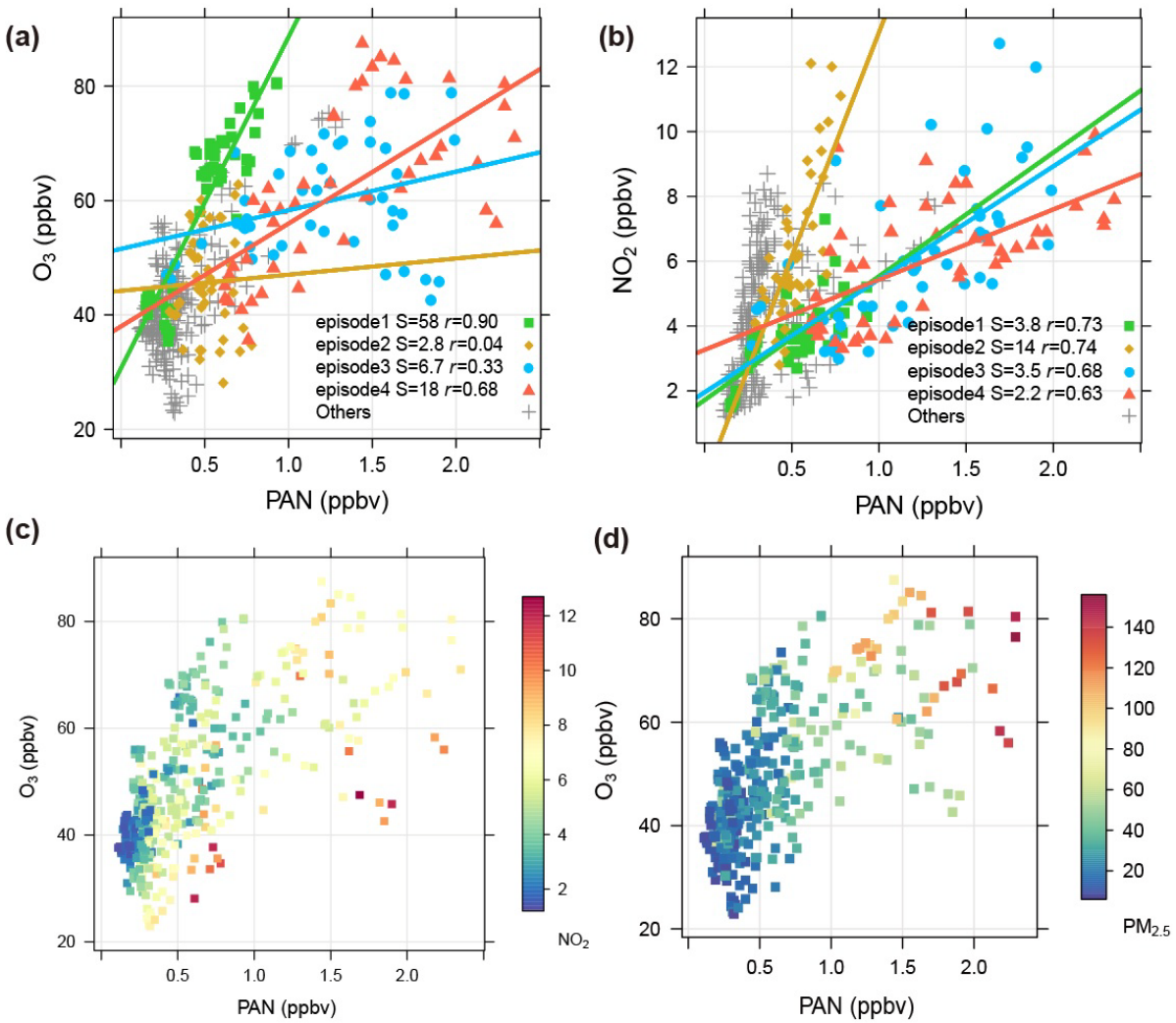
(a)
O3 (ppbv)
PAN (ppbv)
episode1 S=58 r=0.90
episode2 S=2.8 r=0.04
episode3 S=6.7 r=0.33
episode4 S=18 r=0.68
Others
(b)
NO2 (ppbv)
PAN (ppbv)
episode1 S=3.8 r=0.73
episode2 S=14 r=0.74
episode3 S=3.5 r=0.68
episode4 S=2.2 r=0.63
Others
(c)
O3 (ppbv)
PAN (ppbv)
NO2
(d)
O3 (ppbv)
PAN (ppbv)
PM2.5

Figure 5.

708

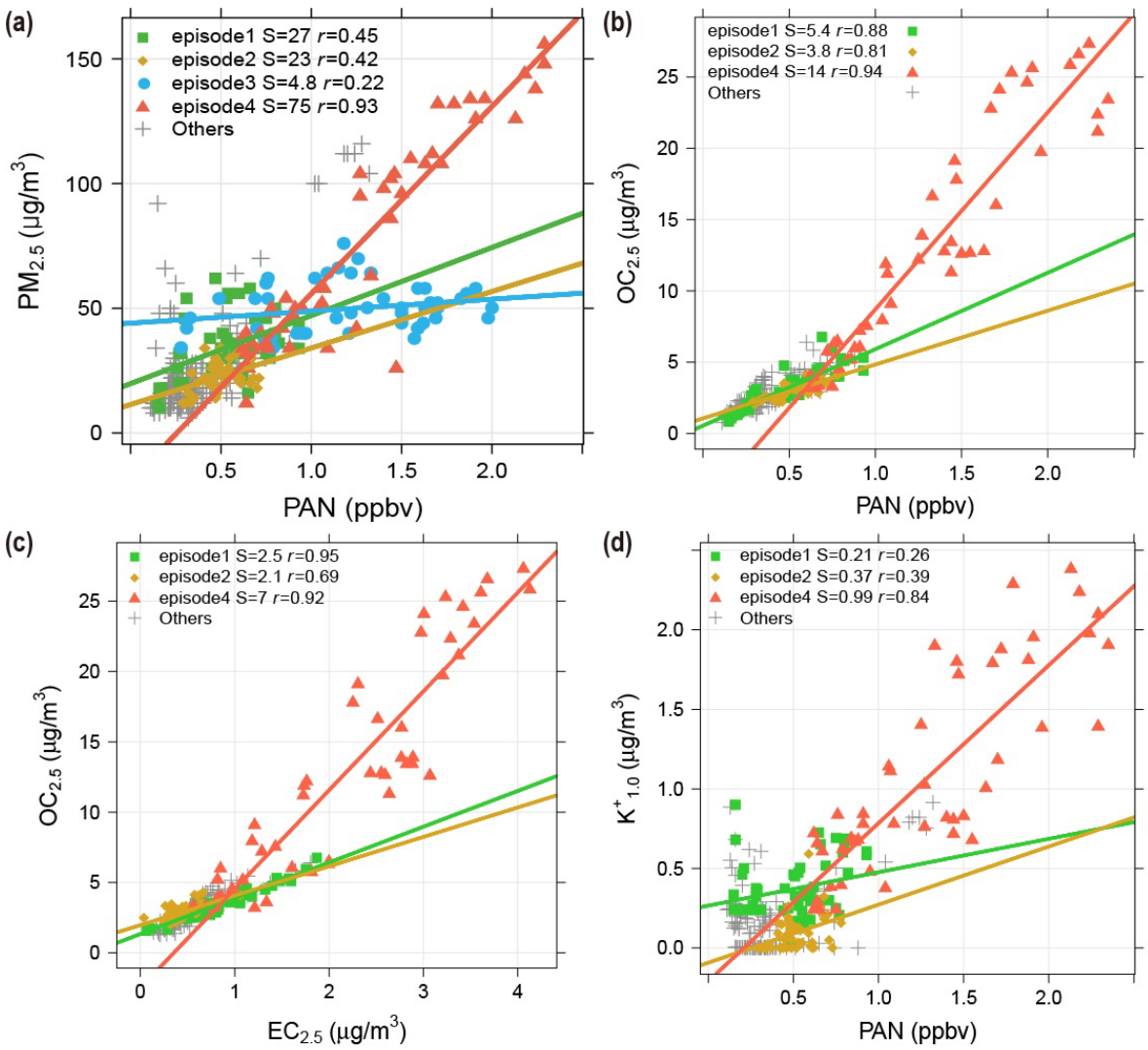


709

710 Figure 6.

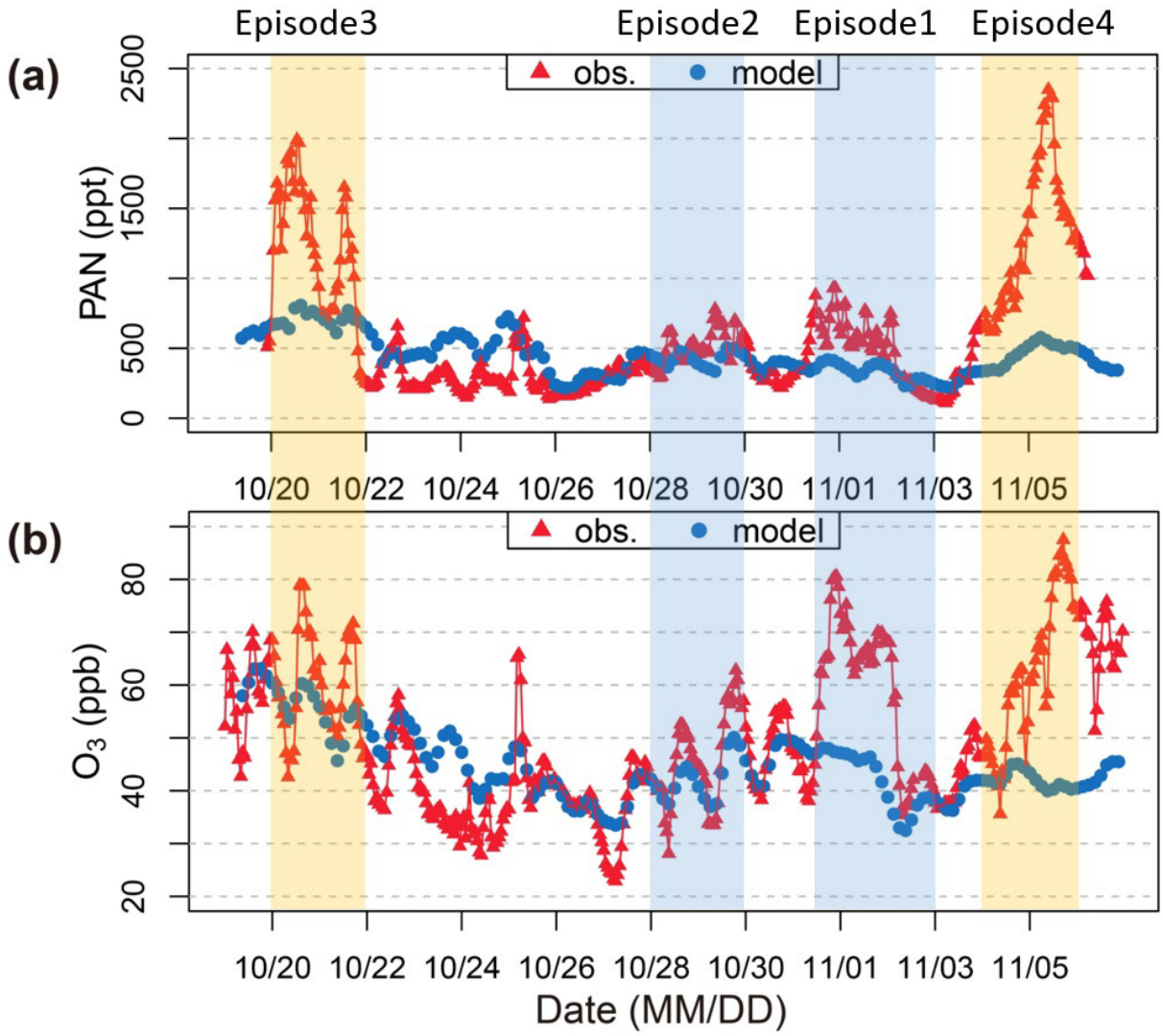


711

712 Figure 7.